

**The Effective Solid Angle Concept and**  
**ANGLE v3.0** Computer Code for  
**Semiconductor Detector Gamma-Efficiency Calculations**  
*– Applicability to In-situ Characterization of Contaminated Sites –*

*S. Jovanovic, A. Dlabac, N. Mihaljevic*

*University of Montenegro  
Centre for Nuclear Competence and  
Knowledge Management  
Podgorica, Montenegro*

# Gamma-Energy Peak Efficiency

In any gamma-spectrometric (quantitative) measurement with semiconductor detectors, the question of **converting the number of counts** - collected by multichannel analyser (MCA) in a full energy peak - **into the activity (concentration)** of the sample/source cannot be avoided.

There are, in principle, three approaches to this issue, as follows.

1) **Relative**, where one tries to **imitate** as good as possible the **source by a standard** (or vice versa), while keeping the same counting conditions for the two. Paid enough care, the result is, in general, so accurate that cannot be surpassed by other methods.

However, we all know what "enough care" means in practice. Combined with the inflexibility in respect with varying source&container parameters (shape, dimensions, material composition), this represents *raison d'être* of the other approaches, as follows.

2) **Absolute** calculations (Monte Carlo methods) yield full energy peak efficiency ( $\varepsilon_p$ ) or total efficiency ( $\varepsilon_{\text{tot}}$ ) for a given counting arrangement.

It is essentially **statistical treatment** of the events which photons undergo - from being emitted by a source atom until the interaction with the detector active body - including the treatment of the so produced electrons, positrons and other subsequent energy carriers.

Absolute approach is beautifully **exact**, on condition that we consider sufficiently large number of incident photons and that we know all the details about

- **source, detector and intercepting layers'** geometrical and compositional data
- **the corresponding photon attenuation coefficients**
- **energy and angle** dependent cross section for various photon interactions with the detector active body, and
- **parameters characterizing electron/positron behaviour** in the latter

At present, inherent statistical uncertainty of Monte Carlo methods, **unsatisfactory manufacturers' detector specifications** and relatively **poor knowledge of the above physical parameters (some of)** are limiting factors for its applicability.

**3) Semiempirical models**, trying to conciliate the previous two. Semiempirical models commonly consist of two parts:

- **experimental** (producing one kind or another of reference efficiency characteristic of the detector) and
- relative-to-this (‘efficiency transfer’ – ET) **calculation of  $\varepsilon_p$**

Inflexibility of the relative method is avoided in this way, as well as the demand for some physical parameters needed in Monte Carlo calculations.

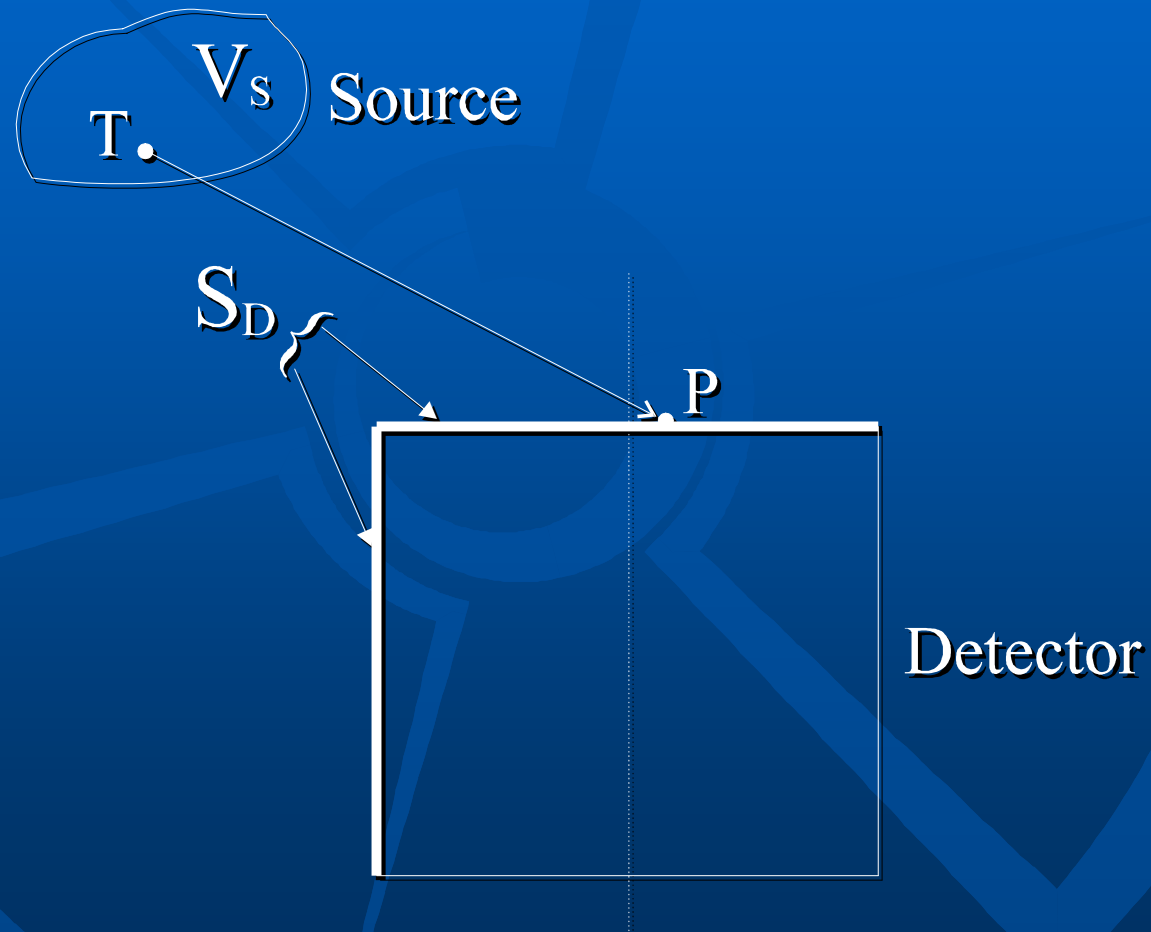
**ET contributes significantly to error compensation in  $\varepsilon_p$ .**

Numerous variations exist within this approach, with emphases either to experimental or to computational part. Most of them simplify (or oversimplify) the physical model behind, i. e. the treatment of

- gamma-attenuation
- geometry and
- detector response

It was shown earlier (**within the development of the k0-NAA method**) that only simultaneous differential treatment of these three factors is essentially justified. This fact is transformed into the concept of the **effective solid angle**  $\bar{\Omega}$  - a calculated value incorporating the three components, and closely related to the detection efficiency.

# Theoretical



To the definition of **the effective solid angle** ( $\bar{\Omega}$ )



# Theoretical

Given a gamma-source and a semiconductor detector, the effective solid angle is defined as:

$$\overline{\Omega} = \int_{V_S, S_D} d\overline{\Omega}$$

with  $V_S$  = source volume,  $S_D$  = detector surface exposed to the source ("visible" by the source) and

$$d\overline{\Omega} = \frac{F_{att} \cdot F_{eff} \cdot \text{TP} \cdot \mathbf{n}_u}{|\text{TP}|^3} d\sigma$$

Here  $T$  is point varying over  $VS$ ,  $P$  point varying over  $SD$ , and  $\underline{nu}$  the external unit vector normal to infinitesimal area  $d\sigma$  at  $S_D$ . Eq. (1) is thus a five fold integral.

Factor  $F_{att}$  accounts for gamma **attenuation** of the photon following the direction  $TP$  out of the detector active zone, while  $F_{eff}$  describes the probability of an energy degradable **photon interaction with the detector** material (i.e. coherent scattering excluded), initiating the detector response.

The two factors include therefore geometrical and compositional parameters of the materials traversed by the photon.

# Theoretical

With  $\varepsilon_p$  being proportional to  $\overline{\Omega}$ , the detection efficiency is found as:

$$\varepsilon_p = \varepsilon_{p,ref} \frac{\overline{\Omega}}{\overline{\Omega}_{ref}}$$

where index "ref" denotes reference counting geometry to which the actual one is relative.

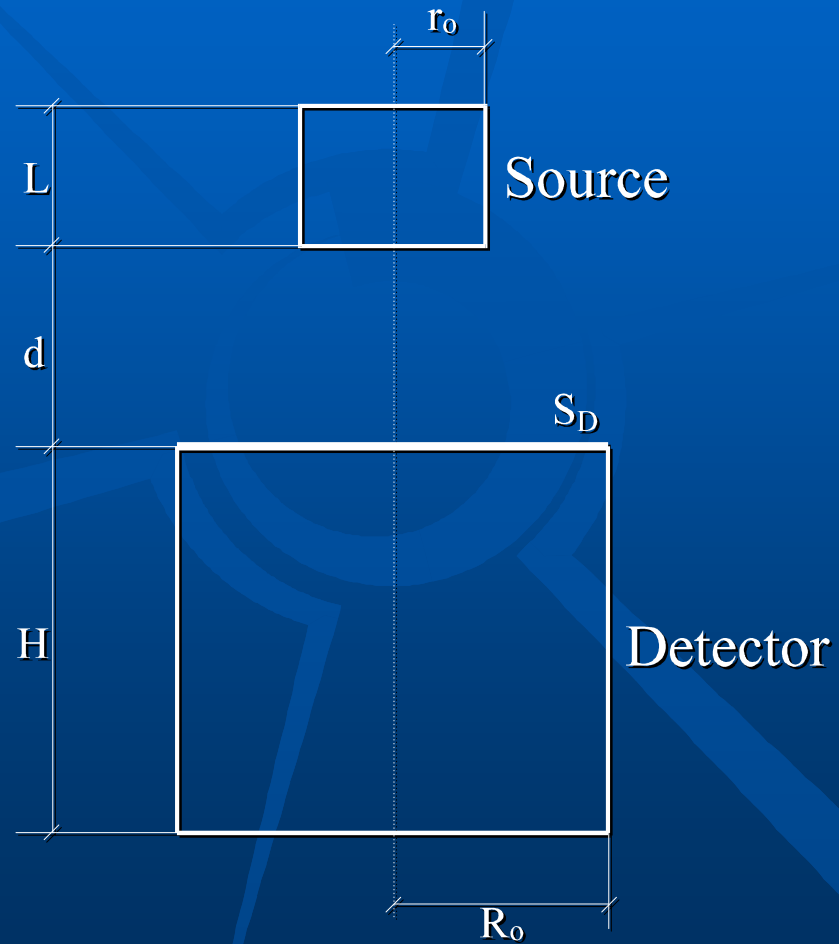
**The above ratio reduces, even significantly, error propagation from input (e.g. detector) data !**

# Theoretical

So as to apply this method the following should be known:

- **reference efficiency curve (REC)**, usually obtained by counting calibrated point sources at a reference distance (e. g. 15-20 cm), and covering gamma-energies ( $E_\gamma$ ) in the region of interest (e. g. 50 -3000 keV); considerable effort should be put in this phase to reach accurate ( $E_\gamma$ ) function, but it pays off in further exploitation;
- **geometrical and compositional data** about
  - source
  - detector
  - intercepting layers (source container and holder, detector end cap and housing, dead layers, etc.);
- **gamma-attenuation coefficients** for all materials involved

# Theoretical



*Cylindrical source ( $r_0 < R_0$ )*

# Theoretical

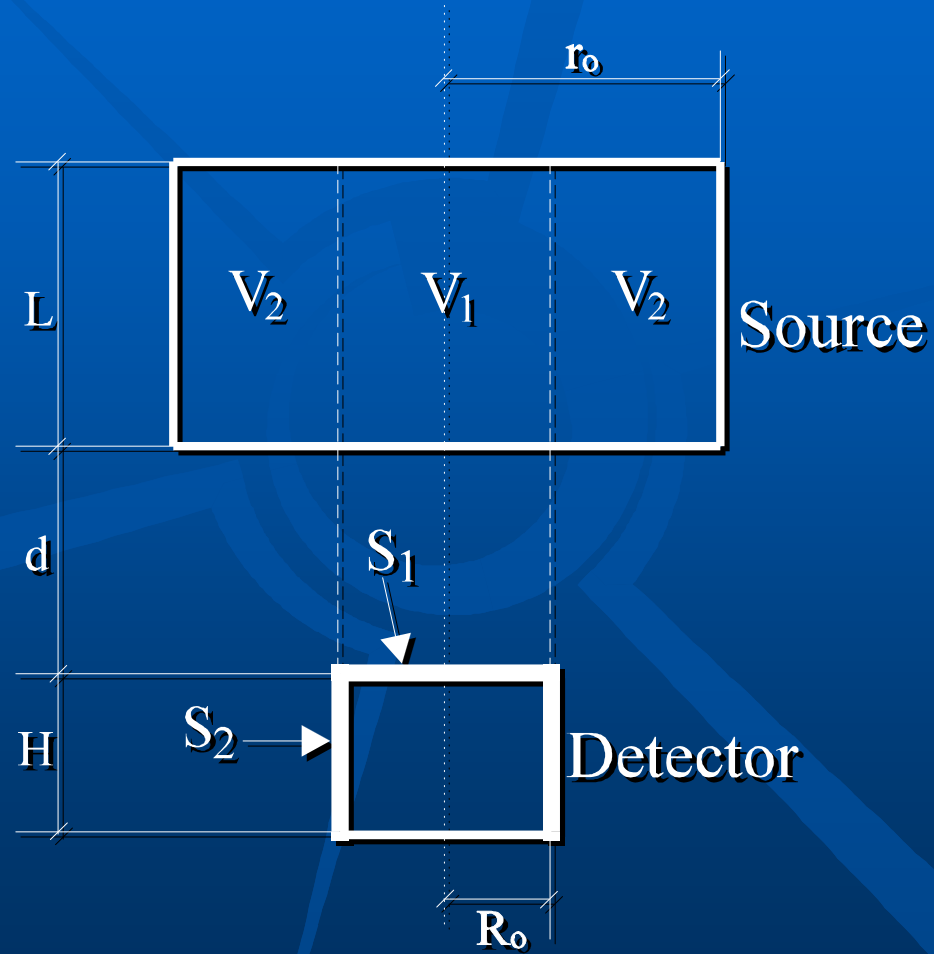
For a cylindrical source coaxially positioned with the detector, and with radius smaller than that of the detector ( $r_0 < R_0$ ):

$$\bar{\Omega} = \frac{4}{r_o^2 L} \int_0^L (d+l) dl \int_0^{r_o} r dr \int_0^\pi d\phi \int_0^{R_o} \frac{F_{att} \cdot F_{eff} \cdot R dR}{\left[ R^2 - 2Rr \cos\phi + r^2 + (d+l)^2 \right]^{3/2}}$$

In the above, five fold integral is reduced to four fold due to axial symmetry. Disk and point sources are included in equation (for  $L=0$ , and  $L=0$ ,  $r_0=0$ , respectively).

**(SOLANG, KAYZERO/SOLCOI)**

# Theoretical



*Cylindrical source ( $r_0 > R_0$ )*

# Theoretical

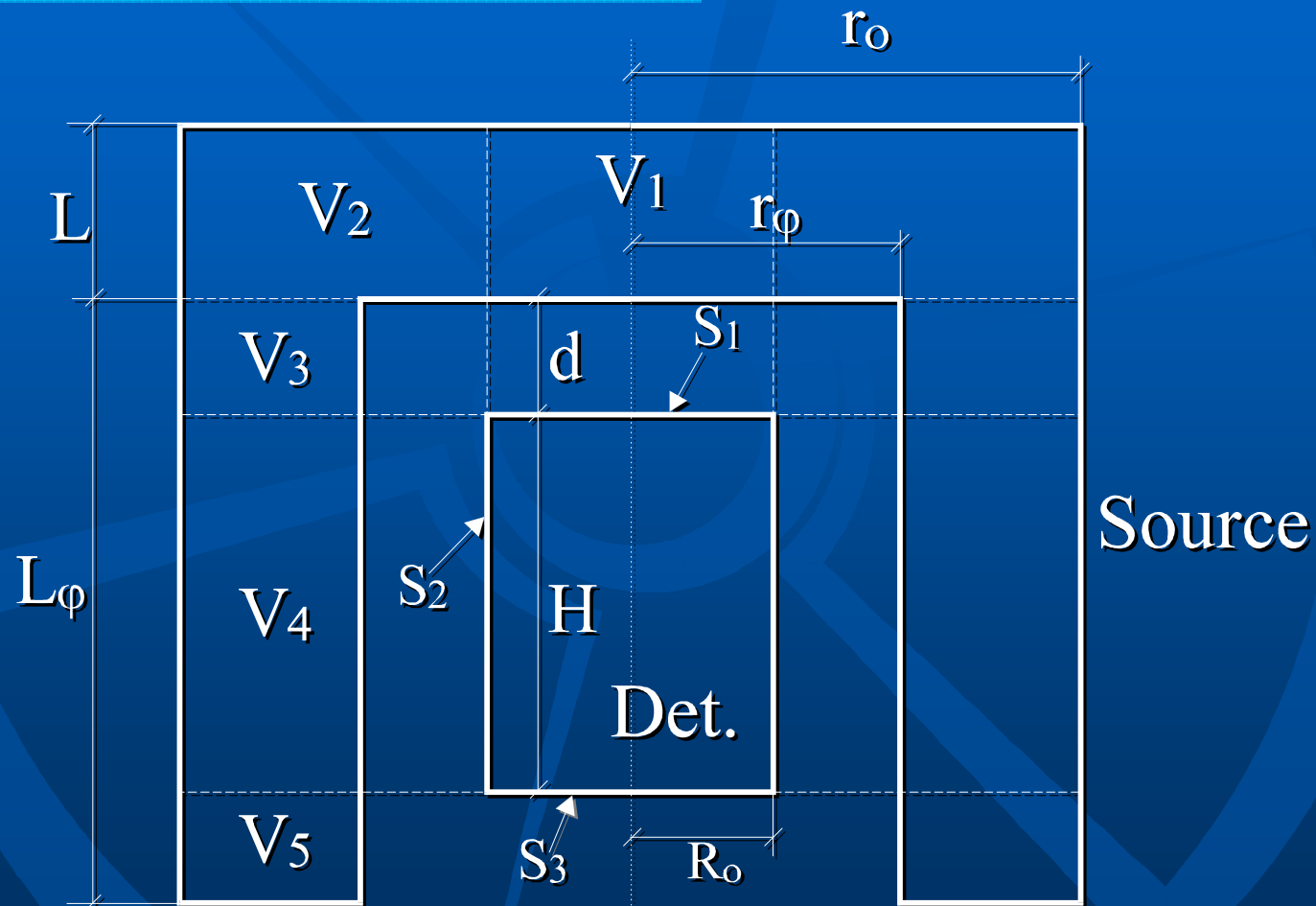
For sources with radii larger than that of the detector ( $r_0 > R_0$ ) we obtain:

$$\begin{aligned}\bar{\Omega} &= \int_{V_1, S_1} d\bar{\Omega} + \int_{V_2, (S_1+S_2)} d\bar{\Omega} = \\ &= \frac{4}{r_o^2 L} \int_0^L (d+l) dl \int_0^{r_o} r dr \int_0^\pi d\phi \int_0^{R_o} \frac{F_{att} \cdot F_{eff} \cdot R dR}{\left[ R^2 - 2Rr \cos\phi + r^2 + (d+l)^2 \right]^{3/2}} + \\ &+ \frac{4R_o}{(r_o^2 - R_o^2)L} \int_0^L dl \int_{R_o}^{r_o} r dr \int_0^{\phi_o} d\phi \int_{-H}^0 \frac{F_{att} \cdot F_{eff} \cdot (r \cos\phi - R_o) dh}{\left[ R_o^2 - 2R_o r \cos\phi + r^2 + (d+l-h)^2 \right]^{3/2}}\end{aligned}$$

with  $\phi_o = \phi_o(r) = \arctg \frac{\sqrt{r^2 - R_o^2}}{R_o}$



# Theoretical



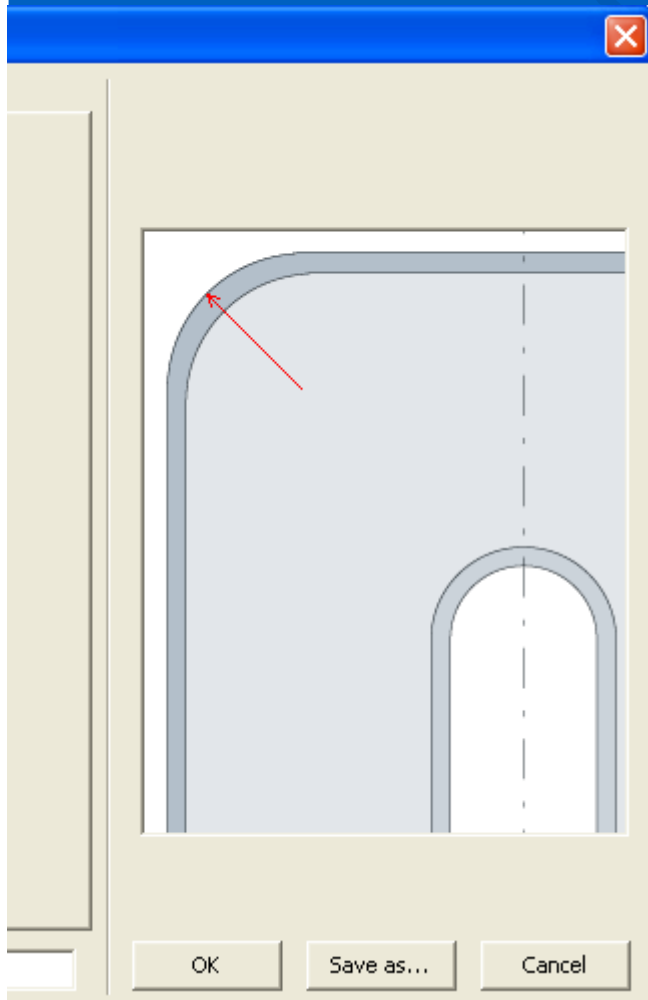
## Marinelli geometry

# Theoretical

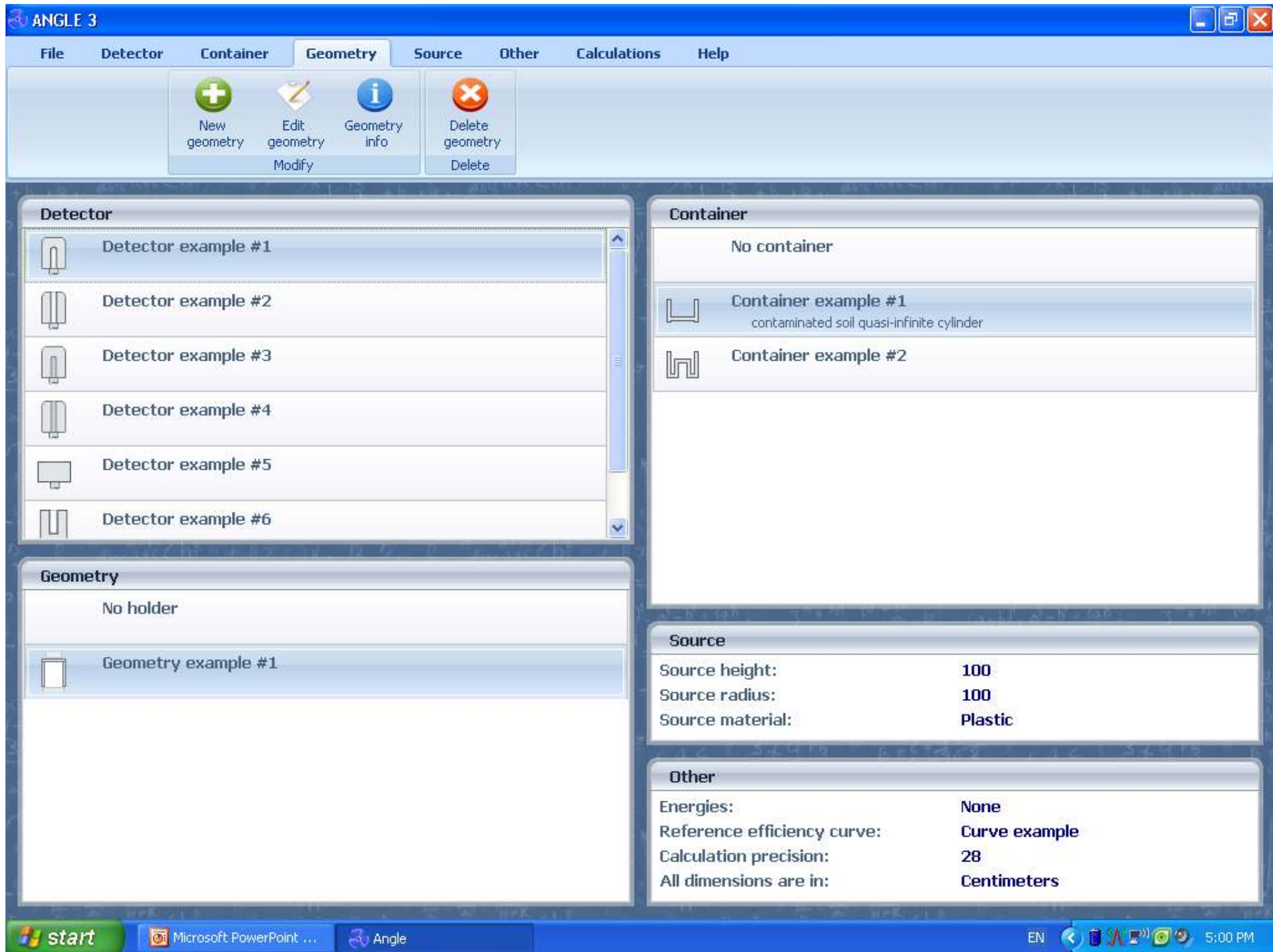
Marinelli geometry can be described as:

$$\begin{aligned}
 \overline{\Omega} = & \int_{(V_1+V_2), S_1} d\overline{\Omega} + \int_{V_2, S_2} d\overline{\Omega} + \int_{V_3, S_1} d\overline{\Omega} + \int_{(V_3+V_4), S_2} d\overline{\Omega} + \int_{V_5, (S_2+S_3)} d\overline{\Omega} = \\
 = & \frac{4}{r_o^2 L + (r_o^2 - r_\phi^2) L_\phi} \int_0^L (d+l) dl \int_0^{r_o} r dr \int_0^\pi d\phi \int_0^{R_o} \frac{F_{att} \cdot F_{eff} \cdot R dR}{[R^2 - 2Rr \cos\phi + r^2 + (d+l)^2]^{3/2}} + \\
 & + \frac{4R_o}{r_o^2 L + (r_o^2 - r_\phi^2) L_\phi} \int_0^L dl \int_{R_o}^{r_o} r dr \int_0^{\phi_o} d\phi \int_{-H}^0 \frac{F_{att} \cdot F_{eff} \cdot (r \cos\phi - R_o) dh}{[R_o^2 - 2R_o r \cos\phi + r^2 + (d+l-h)^2]^{3/2}} + \\
 & + \frac{4}{r_o^2 L + (r_o^2 - r_\phi^2) L_\phi} \int_0^d l dl \int_{r_\phi}^{r_o} r dr \int_0^\pi d\phi \int_0^{R_o} \frac{F_{att} \cdot F_{eff} \cdot R dR}{(R^2 - 2Rr \cos\phi + r^2 + l^2)^{3/2}} + \\
 & + \frac{4R_o}{r_o^2 L + (r_o^2 - r_\phi^2) L_\phi} \int_{d-L\phi}^d dl \int_{r_\phi}^{r_o} r dr \int_0^{\phi_o} d\phi \int_{-H}^0 \frac{F_{att} \cdot F_{eff} \cdot (r \cos\phi - R_o) dh}{[R_o^2 - 2R_o r \cos\phi + r^2 + (l-h)^2]^{3/2}} + \\
 & + \frac{-4}{r_o^2 L + (r_o^2 - r_\phi^2) L_\phi} \int_{d-L\phi}^{-H} (l+H) dl \int_{r_\phi}^{r_o} r dr \int_0^\pi d\phi \int_0^{R_o} \frac{F_{att} \cdot F_{eff} \cdot R dR}{[R^2 - 2Rr \cos\phi + r^2 + (l+H)^2]^{3/2}} \quad (6)
 \end{aligned}$$

# Accounting for detector crystal **edge rounding** ("bulettizing")



$$\begin{aligned}
 \bar{\Omega} = & \frac{4}{r_0^2 L + (r_0^2 - r_\phi^2) \angle \varphi} \int_0^L dl \int_0^{r_0} r dr \int_0^\pi d\theta \int_0^{R_0 - \rho} F_{att} F_{eff} F_1(T, P_{S_1}) R dR + \\
 & + \frac{4}{r_0^2 L + (r_0^2 - r_\phi^2) \angle \varphi} \int_0^L dl \int_0^{r_0} r dr \int_0^\pi d\theta \int_{R_0 - \rho}^{R_0} F_{att} F_{eff} F_{13}(T, P_{S_1}) R dR + \\
 & + \frac{4 R_0}{r_0^2 L + (r_0^2 - r_\phi^2) \angle \varphi} \int_0^L dl \int_{R_0}^{r_0} r dr \int_0^{\theta_0} d\theta \int_{-H}^{R_0 - \rho} F_{att} F_{eff} F_2(T, P_{S_2}) dh + \\
 & + \frac{4 R_0}{r_0^2 L + (r_0^2 - r_\phi^2) \angle \varphi} \int_0^L dl \int_{R_0}^{r_0} r dr \int_0^{\theta_0} d\theta \int_{-\rho}^0 F_{att} F_{eff} F_{23}(T, P_{S_2}) dh + \\
 & + \frac{4}{r_0^2 L + (r_0^2 - r_\phi^2) \angle \varphi} \int_0^d dl \int_{r_\phi}^{r_0} r dr \int_0^\pi d\theta \int_0^{R_0 - \rho} F_{att} F_{eff} F_3(T_m, P_{S_1}) R dR + \\
 & + \frac{4}{r_0^2 L + (r_0^2 - r_\phi^2) \angle \varphi} \int_0^d dl \int_{r_\phi}^{r_0} r dr \int_0^\pi d\theta \int_{R_0 - \rho}^{R_0} F_{att} F_{eff} F_{33}(T_m, P_{S_1}) R dR + \\
 & + \frac{4 R_0}{r_0^2 L + (r_0^2 - r_\phi^2) \angle \varphi} \int_{d-L_\varphi}^d dl \int_0^{r_0} r dr \int_0^{\theta_0} d\theta \int_{-H}^{-\rho} F_{att} F_{eff} F_4(T_m, P_{S_2}) dh + \\
 & + \frac{4 R_0}{r_0^2 L + (r_0^2 - r_\phi^2) \angle \varphi} \int_{d-L_\varphi}^d dl \int_0^{r_0} r dr \int_0^{\theta_0} d\theta \int_{-\rho}^0 F_{att} F_{eff} F_{43}(T_m, P_{S_2}) dh - \\
 & - \frac{4}{r_0^2 L + (r_0^2 - r_\phi^2) \angle \varphi} \int_{d-L_\varphi}^{-H} dl \int_{r_\phi}^{r_0} r dr \int_0^\pi d\theta \int_0^{R_0} F_{att} F_{eff} F_5(T_m, P_{S_4}) R dR
 \end{aligned}$$



# detector data input

**Detector change** [X]

Detector | Window | Antimicrophonic shield | End-cap | Vacuum | Housing

Detector name:

Detector type:

Detector height:

Detector radius:

Bulletizing radius (0 = none):

Core top type: ☐ Flat ☒ Rounded

Core height:

Core radius:

Inactive Ge top thickness:

Inactive Ge side thickness:

Contact top thickness:

Contact side thickness:

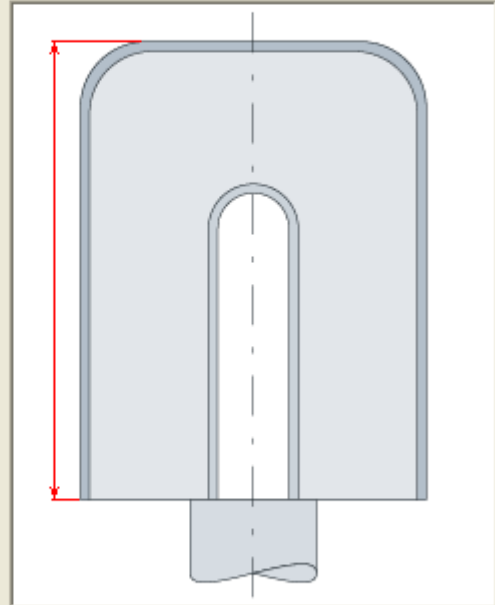
Contact material:

Contact pin radius:

Contact pin material:

Detector description:

OK Save as... Cancel



# source container data input

**Container change** [X]

Container | Container coatings

Container name:

Container type:

Container inside radius:

Marinelli cavity radius:

Marinelli cavity depth:

Marinelli upper bottom thickness:

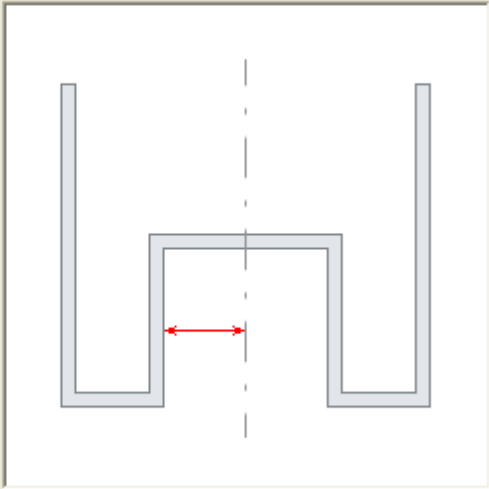
Marinelli inner side thickness:

Marinelli lower bottom thickness:

Container material:

Container description:

OK Save as... Cancel



The diagram shows a cross-section of a Marinelli container. It features a central horizontal cavity with a vertical dashed line indicating the center of symmetry. The container walls are represented by thick grey lines. A red double-headed arrow is positioned below the central cavity, indicating its width. The diagram illustrates the geometric parameters defined in the input fields, such as the cavity radius and the various thicknesses of the container walls.

# geometry data input

**Geometry change** [X]

Geometry | Additional intercepting layers

Geometry name:

Holder outer radius:

Holder cap thickness:

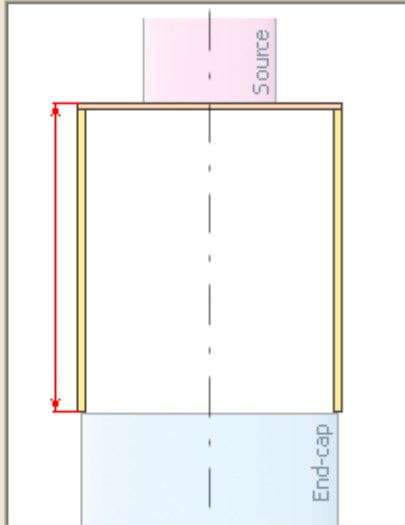
Holder cap material:

Holder wall thickness:

Holder wall material:

Holder height:

Geometry description:



OK Save as... Cancel

# reference efficiency curve data input

**Reference efficiency curve**

Experimental points  
Number of points: 25

$E_\gamma$	$\epsilon_{p,ref}$
53,17	9,78E-5
80,88	0,0003423
121,78	0,0004714
122,06	0,0004703
136,46	0,0004707
160,61	0,000473
223,23	0,0004043
244,7	0,0004049
276,4	0,0003689
302,8	0,0003441
344,28	0,0003253
355,95	0,0003137
383,78	0,0002948
411,11	0,0002624
444	0,0002757
661,65	0,0002027

Energy regions  
Number of regions: 3

[	keV	,	keV	]	Polynom order
50		300			3
300		700			1
700		2000			1

Detector  
Detector name: Detector example #1

Container  
Container: Curve example - Container

Geometry  
Geometry: Curve example - Geometry

Source  
Source height: 10.72  
Source radius: 4.31  
Source material: Water

$\epsilon_{p,ref}$

$E_\gamma, \text{keV}$

Reference efficiency curve name: Curve example

Reference efficiency curve description:

New curve Load curve from file Import from GammaVision OK Cancel



# output data file

**Output** [X]

Output file: **Output example.out**

Detector name: **Detector example #1** [i]

Container name: **Container example #1** [i]

Geometry name: **Geometry example #1** [i]

Source height: **5.3**

Source radius: **1.1**

Source material: **Water** [i]

Number of energies: **8** [i]

Reference efficiency curve: **Curve example** [i]

Gauss coefficient order: **10**

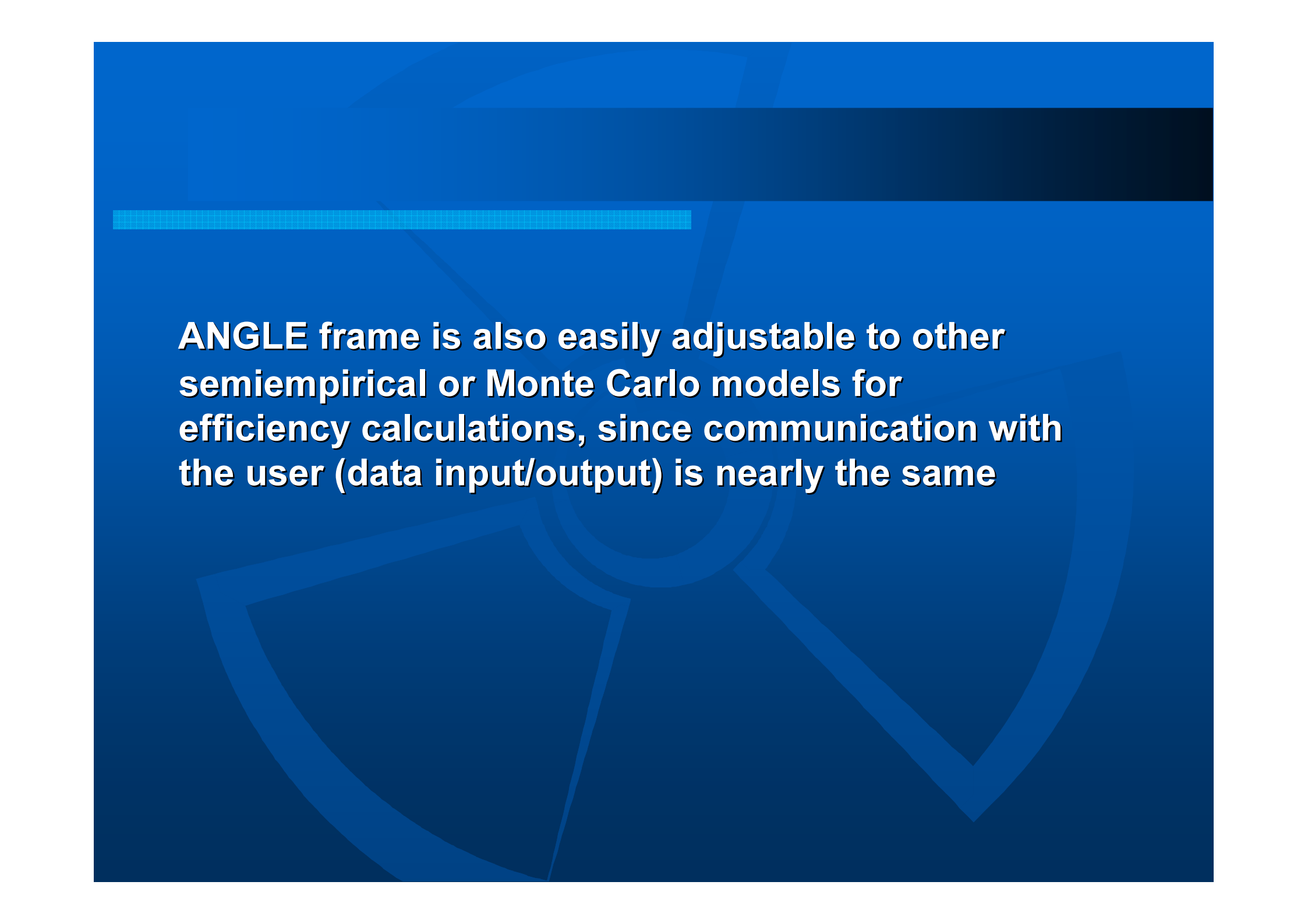
Calculation duration: **0:00**

---

Calculated values:

$E_\gamma$	$\Omega_{\text{eff}}$	$\epsilon_p$
60	0.0338829265648614	0.00108880718600845
90	0.0425408892554379	0.00276342161407703
150	0.0451293445324021	0.00345571059953243
250	0.0440890139553926	0.00279202312864821
450	0.0419038351171812	0.00200148519534467
700	0.0401160315285273	0.0015551848764458
1200	0.0369330953298705	0.00111203872929305

[Copy icon] Copy to clipboard [GammaVision icon] Export to GammaVision [OK]

The background is a solid blue color with abstract, darker blue geometric shapes, including a large circle and several triangles, some of which are outlined. A horizontal bar with a light blue grid pattern is positioned near the top left.

**ANGLE frame is also easily adjustable to other semiempirical or Monte Carlo models for efficiency calculations, since communication with the user (data input/output) is nearly the same**

# Possibilities

- Any type of commercial semiconductor detector (HPGe, Ge-Li, well, LEPD)
- Practically any type of typical gamma source (point, disk, cylinder, Marinelli)
- Extraordinary flexible and user-friendly 32-bit Windows application

# Main Advantages:

- Broad application range
- High accuracy
- Easy data manipulation
- Short computation times
- Flexibility
- Teaching/training aspect
- No detector “factory characterization”

When assigning uncertainties to ANGLE calculation results, several **uncertainty-contributing components** should be distinguished, **originating from**

- Detector manufacturer
- ANGLE user and
- ANGLE software itself. These include:

- **detector data**, supplied by the manufacturer
- **geometrical and compositional** (chemical) data of the source, its container vessel and intercepting layers (between the source and the detector), introduced by the user
- **reference efficiency curve**, created or chosen by the user
- **mathematical model and calculation method** applied (ANGLE)
- **gamma-attenuation coefficients** and other physical/chemical parameter data used in calculations (ANGLE)

# Testing Efficiency Transfer Codes for Equivalence

(paper submitted to Appl. Rad. Isot.)

*T. Vidmar (a), N. Çelik (a,b), N. Cornejo Díaz (c), A. Dlabac (d),  
O. B. Ewa (e), J. A. Carrazana González (c), M. Hult (a), S. Jovanović (d),  
M-C. Lépy (f), N.Mihaljević (d), O. Sima, (g), F. Tzika (h),  
M. Jurado Vargas (i), T. Vasilopoulou (h, j), G. Vidmar (k)*

- (a) European Commission, JRC, IRMM, Geel, Belgium
- (b) Karadeniz Technical University, Trabzon, Turkey
- (c) Centro de Protección e Higiene de las Radiaciones, La Habana, Cuba
- (d) University of Montenegro, Podgorica, Montenegro
- (e) Ahmadu Bello University, Zaria, Nigeria
- (f) Commissariat à l'Énergie Atomique, Gif sur Yvette Cedex, France
- (g) Bucharest University, Bucharest, Romania
- (h) National Centre for Scientific Research 'Demokritos', Athens, Greece
- (i) University of Extremadura, Badajoz, Spain
- (j) National Technical University of Athens, Athens, Greece
- (k) Institute for Rehabilitation, Ljubljana, Slovenia

Table 4: The various combinations of the codes, their types and the ET implementations considered in the study

Computer Code	ET Implementation		Code Type	
	FEPE	ET	Specialized	General
ANGLE		x	x	
EFFTRAN		x	x	
DETEFF 4.2	x	x	x	
EGS4	x			X
GEANT 3.21	x	x		X
GESPECOR 4.2	x		x	
MCNP4C	x			X
MCNPX	x			X
PENELOPE 2003	x			X
PENELOPE 2008	x			X
PENELOPE PENCYL	x			X
ETNA		x	x	
MCNPX	x			X



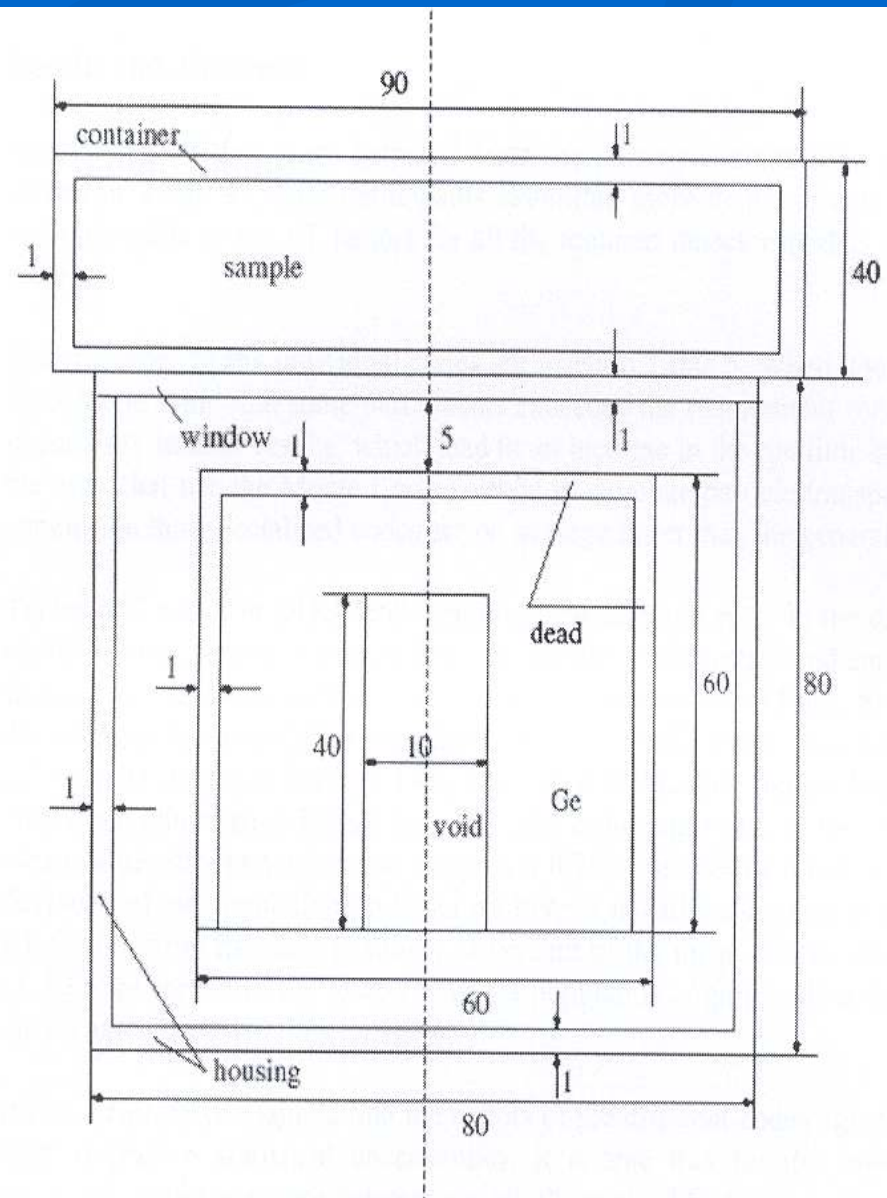


Figure 1: A schematic presentation of the setup for the case of the soil sample and the p-type detector model.

**Efficiency transfer (ET)** from voluminous source  
(large cylinder, aquatic solution) to:

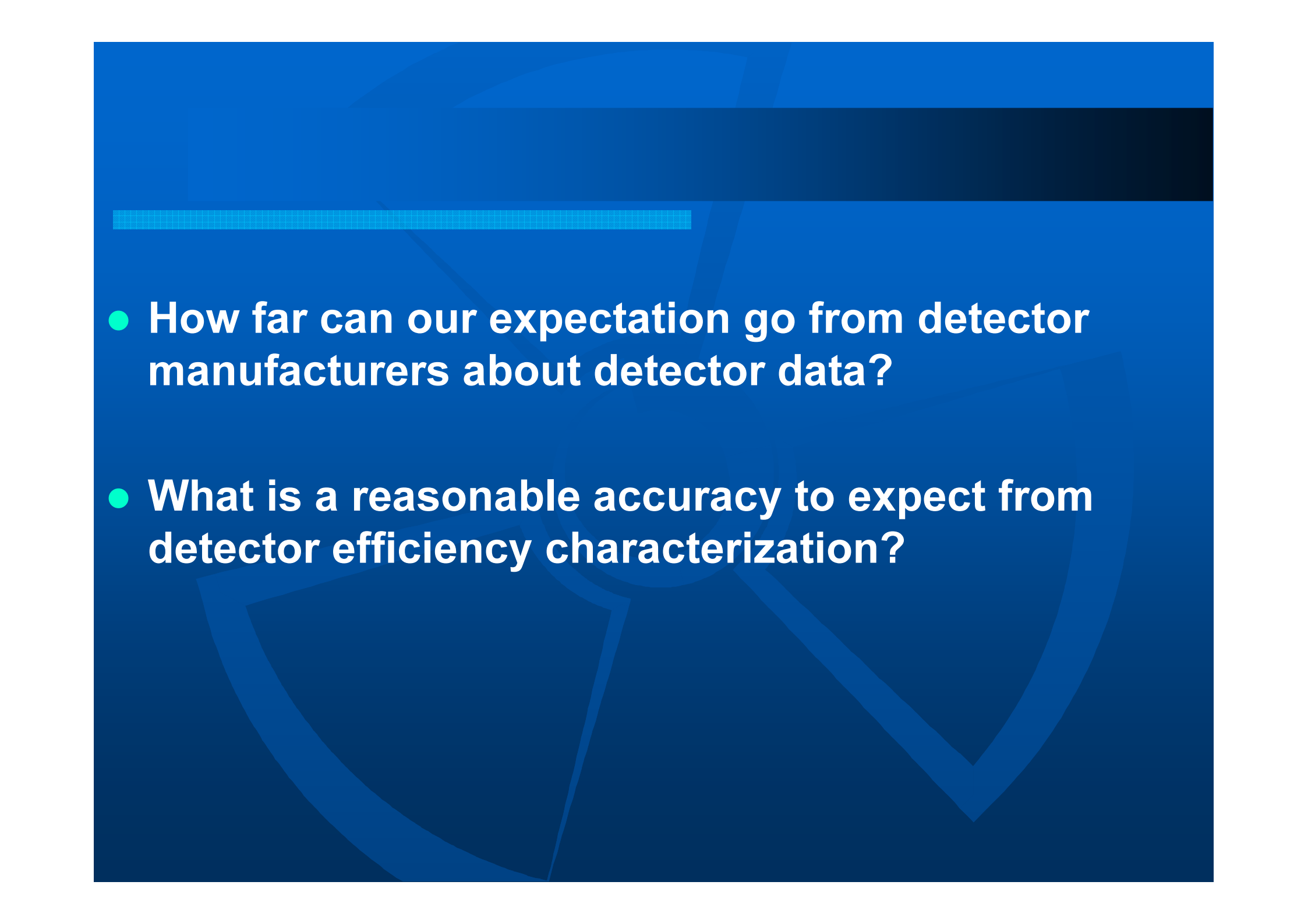
- Point source
- Large disc source (air filter paper)
- Cylinder (quartz matrix)
- n-type and p-type detectors
- Energy range 20 – 2000 keV

Table 7: Standard deviation of the population of the ET factors, as percent of its mean. The value exceeding 2% is marked in bold. The averaging and the standard deviation calculation were done over all the data sets (see text).

Energy	Point A	Point B	Soil A	Soil B	Filter A	Filter B
20		1.4		<b>2.5</b>		1.2
45	0.5	0.9	0.9	0.5	0.9	0.8
60	0.6	0.5	0.9	0.9	1.0	0.5
80	0.6	0.4	0.9	0.7	0.8	0.5
120	0.5	0.4	0.7	0.5	0.6	0.6
200	0.7	0.7	0.6	0.6	0.6	0.8
500	0.8	0.9	0.8	0.3	0.6	0.9
1000	0.7	1.1	0.5	0.5	0.8	0.9
2000	0.7	1.0	0.7	0.6	0.8	0.8

Table 8: The maximum deviation of the population of the ET factors from its mean, as percent of the mean. Values exceeding 2% are marked in bold.

Energy	Point A	Point B	Soil A	Soil B	Filter A	Filter B
20	-	<b>3.1</b>	-	<b>7.6</b>	-	3.4
45	1.2	1.7	<b>3.1</b>	1.3	<b>2.2</b>	1.4
60	1.2	1.1	1.9	<b>2.3</b>	<b>2.5</b>	1.0
80	1.2	1.0	2.0	1.6	2.0	1.1
120	0.9	0.8	1.8	1.6	1.2	1.1
200	1.1	1.4	1.2	1.6	1.2	1.4
500	1.4	1.9	1.7	0.5	1.1	1.5
1000	1.6	2.0	0.9	1.2	1.4	1.5
2000	1.9	1.9	1.5	0.9	1.4	1.3

- 
- **How far can our expectation go from detector manufacturers about detector data?**
  - **What is a reasonable accuracy to expect from detector efficiency characterization?**

Resolution -        keV (FWHM)  
 -        keV (FWTM) @ 1.33 MeV  
 -        keV (FWHM) @         
 -        keV (FWTM) @         
 Peak/Compton -       :1

Cryostat Description or Drw. No. if special Vertical dipstick, type 7500

## 6.2 PHYSICAL/PERFORMANCE DATA

Date: November 29, 1982

Actual performance of this detector when tested is given below. Digital printouts are also enclosed in the rear envelope of the instruction manual.

Geometry Coaxial one open end, closed end facing window.

Diameter 49.4 mm

P-core Diameter 8 mm

Length 48 mm

P-core Length 25 mm

Weight 480 gm

Distance from window 5 mm

Active area facing window 18.7 cm<sup>2</sup>

Thickness of n-layer 0.3 mm

## LEAKAGE CURRENT AND CAPACITANCE

Volts	nAmp	pf
100	0.010	279
200	0.010	220
300		
400		
500	0.010	160

Volts	nAmp	pf
1000	0.010	111
1500	0.010	81
2000	0.010	66
2500	0.018	55
3000	0.031	50

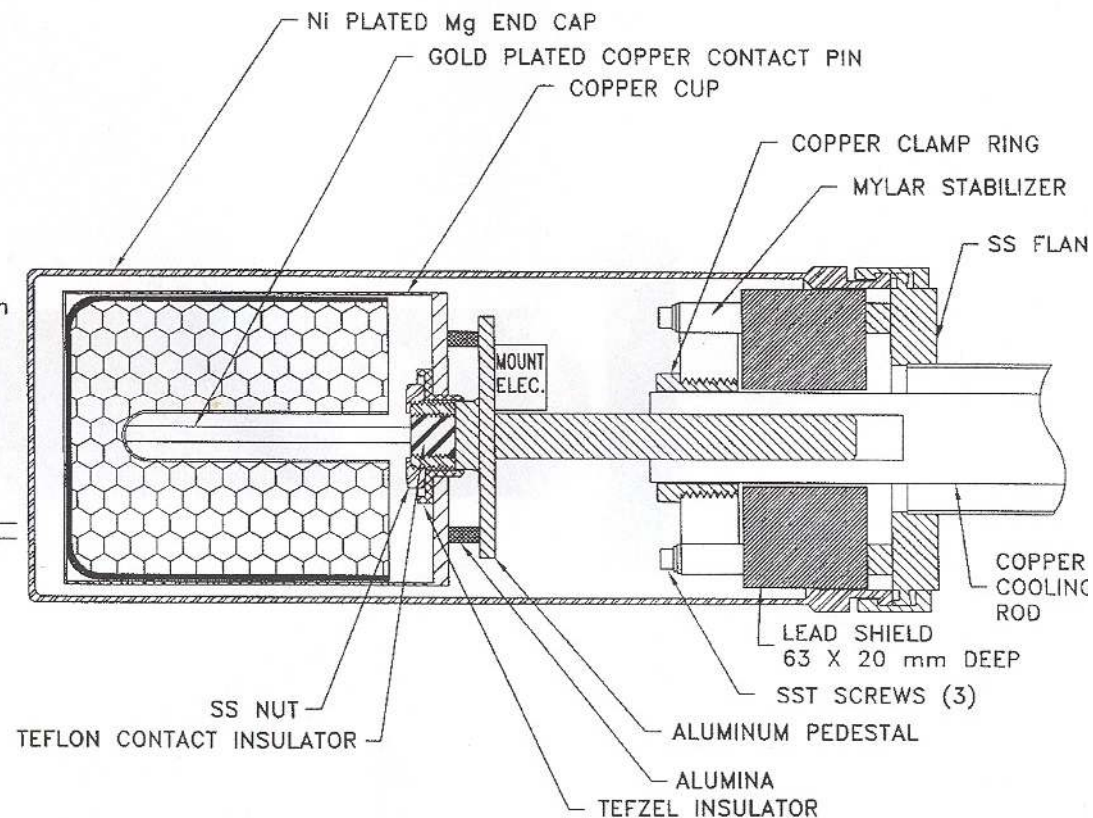
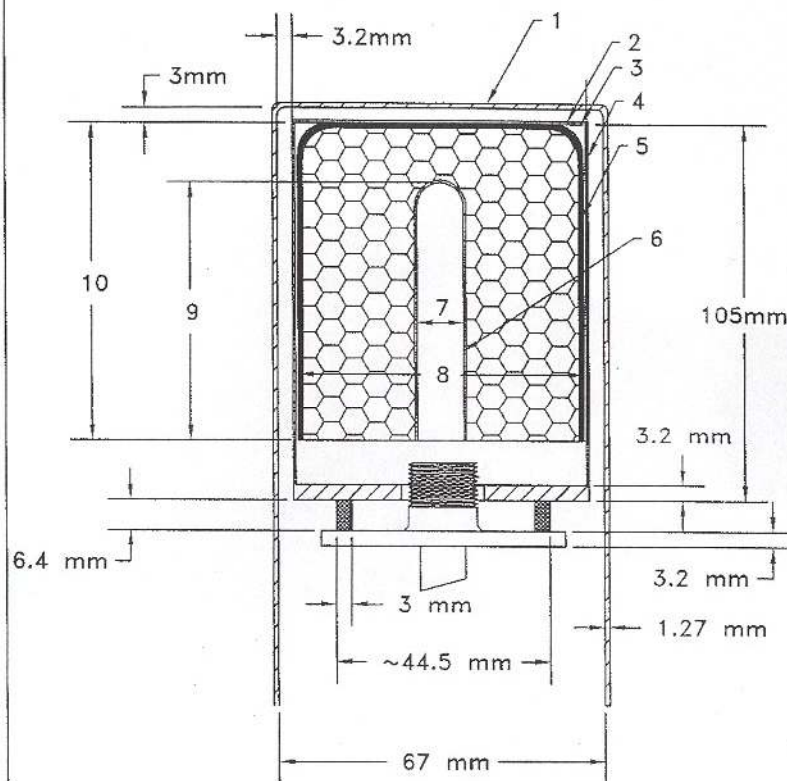
Volts	nAmp	pf
3500	0.040	37
4000	0.050	35
4500	0.063	30
5000	0.068	26

Recommended Operating Voltage: (+) 5000 V

## RESOLUTION AND EFFICIENCY

Isotope	Co <sup>57</sup>	Cs <sup>137</sup>	Co <sup>60</sup>	Th <sup>223</sup>
Energy (keV)	122	662	1332	2614
FWHM (keV)			1.87	





1. Ni plated Mg	1.27 mm
2. MYLAR	0.025 mm
3. ALUMINUM FOIL	0.025 mm
4. ALUMINUM CUP	0.50 mm
5. LITHIUM CONTACT	0.9 mm
6. BORON CONTACT	0.3 microns
7. HOLE DIAMETER	8.9 mm
8. CRYSTAL DIAMETER	59 mm
9. HOLE LENGTH	66.3 mm
10. CRYSTAL LENGTH	80.1 mm

**EG&G ORTEC**

100 MIDLAND ROAD, OAK RIDGE, TENNESSEE 37831

**MATERIALS & DIMENSION  
DETECTOR # 38-P40896**

DRAFTER DLS 12-17-98	DATE 12-17-98	RESP ENG APP DATE	REFERENCE/USED ON
CHECKED	DESIGN ENGR	PROJECT	
MFG APPROVAL	DATE	DRAWING NO.	

- Accuracy of detector specifications is limited by the technological process of their production (dead layer, vacuum, crystal impurities, crystal tilt/shift, ...)
- Even two “identical” detectors from the production line may exhibit significantly different response to gamma-radiation
- Major positive impact is due to partial canceling of input uncertainties for reference and actual counting geometry  
(ET error compensation)

- If not satisfied with detector data, **more than one reference efficiency curve can be produced for the same detector** – so as to closer match the actual samples to the most similar reference one (this option is valid rather for environmental monitoring than for k0-NAA), e.g.
  - two point-source ref. eff. curves (0 cm and 20 cm)
  - one cylinder ref. eff. curve
  - one Marinelli ref. eff. curve
- Uncertainty should be estimated for each case separately, since depending on many factors (energy, geometry, input data reliability, ...)
- Eventually , “uncertainty budget” shows that the best expected combined  $\varepsilon_p$  uncertainty would be:
  - **1-2% for point sources**
  - **3-4% for cylindrical source**
  - **5-7% for Marinelli**( <100 keV and >2000 keV: less reliable)

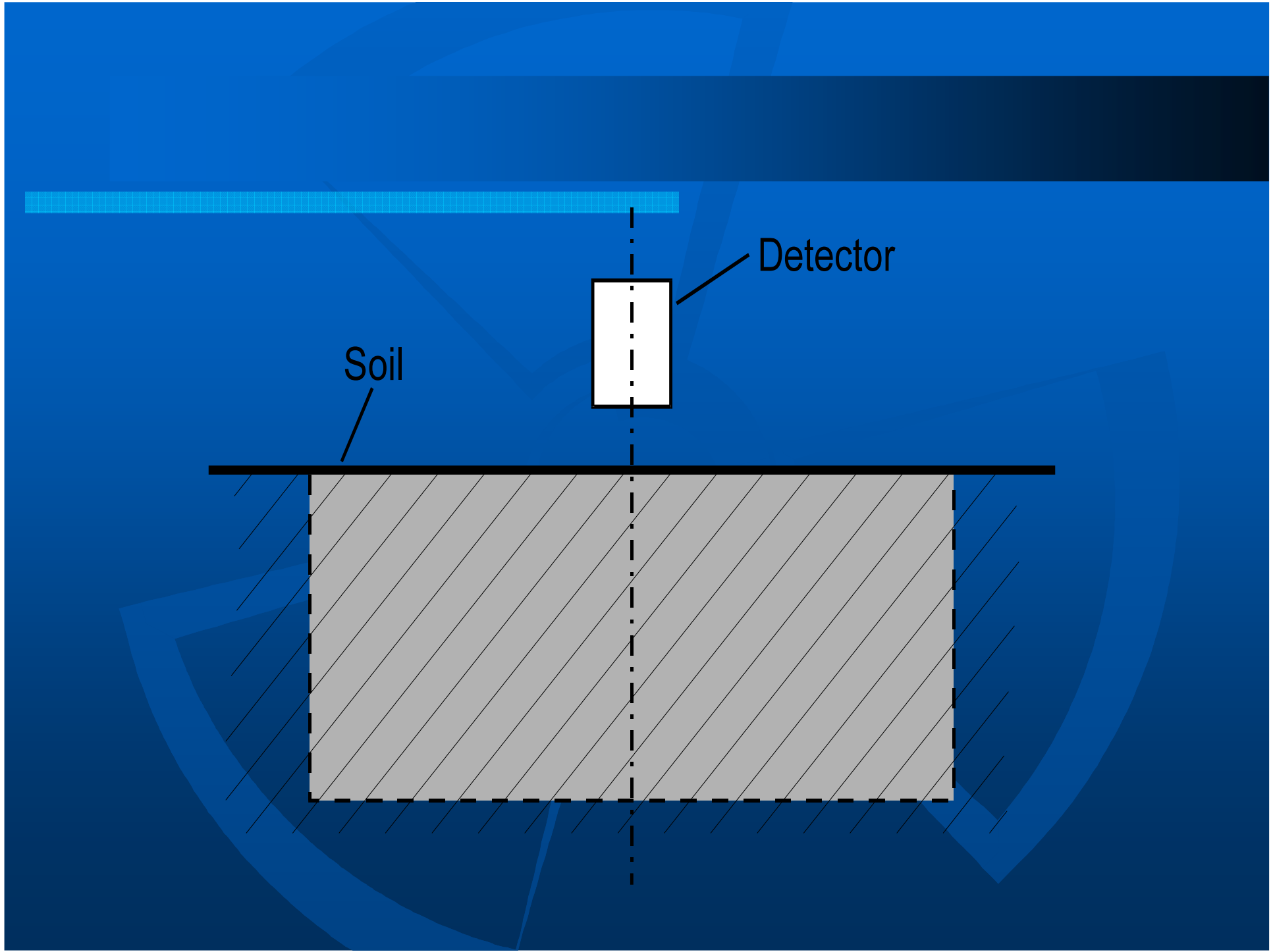




- Applicability to in-situ characterization of contaminated sites
- ANGLE is readily applicable to radioactivity measurements in the environment. Several possibilities are straightforwardly at user's disposal
- Regular" radioactivity measurements of
  - **voluminous (solid or liquid) samples** collected at contaminates sites (either in cylindrical or Marinelli beakers), or
  - **filters** collecting air radioactivity by means of air pumps ("disc" sources).
- ANGLE supports these cases directly through combination of appropriate entries in *Source* and *Container* windows. Activity (A) of a particular nuclide is then simply derived from ANGLE-calculated full-energy detection efficiency and net gamma-peak area ( $N_p$ ) recorded by multichannel analyzer (MCA) during counting time  $t_m$  :

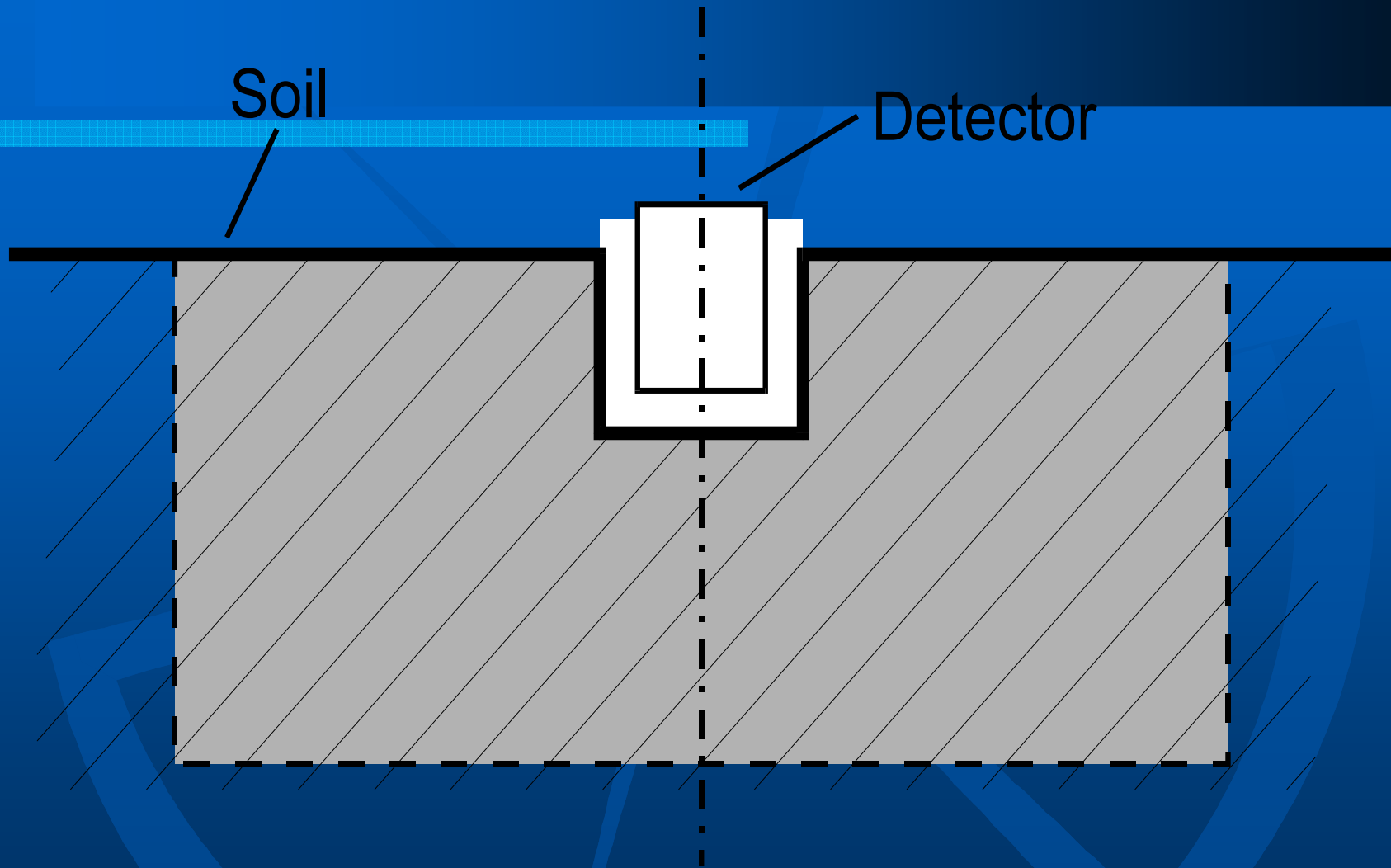
$$A \cdot \epsilon_p = N_p / t_m$$

- Soil radioactivity can be measured by positioning the detector towards the ground or in a hole. These cases correspond to infinite cylinder and infinite Marinelli geometry, respectively. In practice, however, only limited area relatively close to the detector contributes relevantly to the measurement – outside that area the contribution is negligible, either because of the distance or attenuation, or both. 1m source radius (cylinder or Marinelli) usually is good enough approximation.
- Note this model assumes radioactivity to be homogeneously distributed in the soil. An illustration of data entry for quasi-infinite cylindrical source is given.



Soil

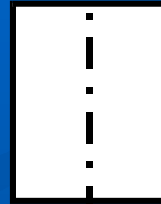
Detector



- In case of surface contamination infinite soil surface can be approximated by a large, finite disc. When surface radioactivity migrates to within certain depth into the soil, slab geometry can be applied. This is, in effect, a large thin cylinder from ANGLE calculations standpoint.
- Note that previous example (surface contamination) is, in mathematical terms, a special case of this one



Detector

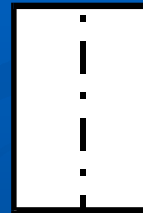


Infinite soil slab

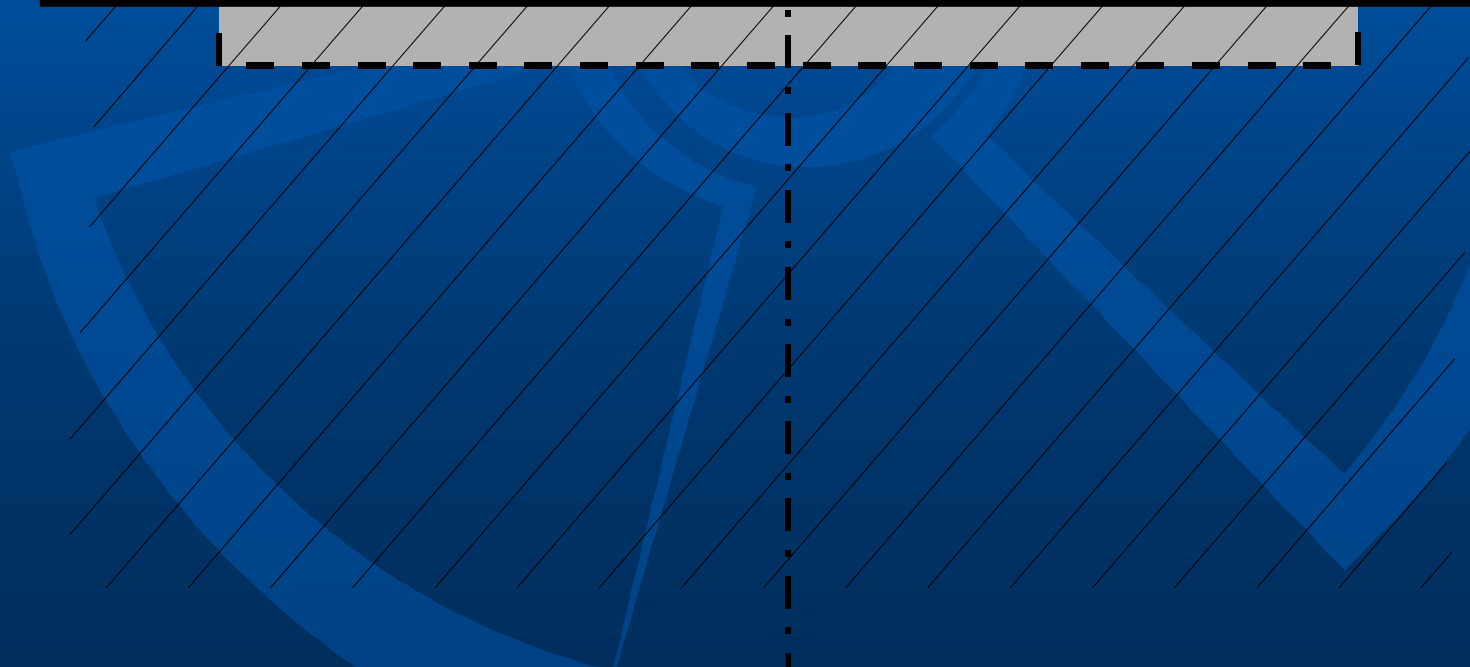




Detector



Finite soil slab

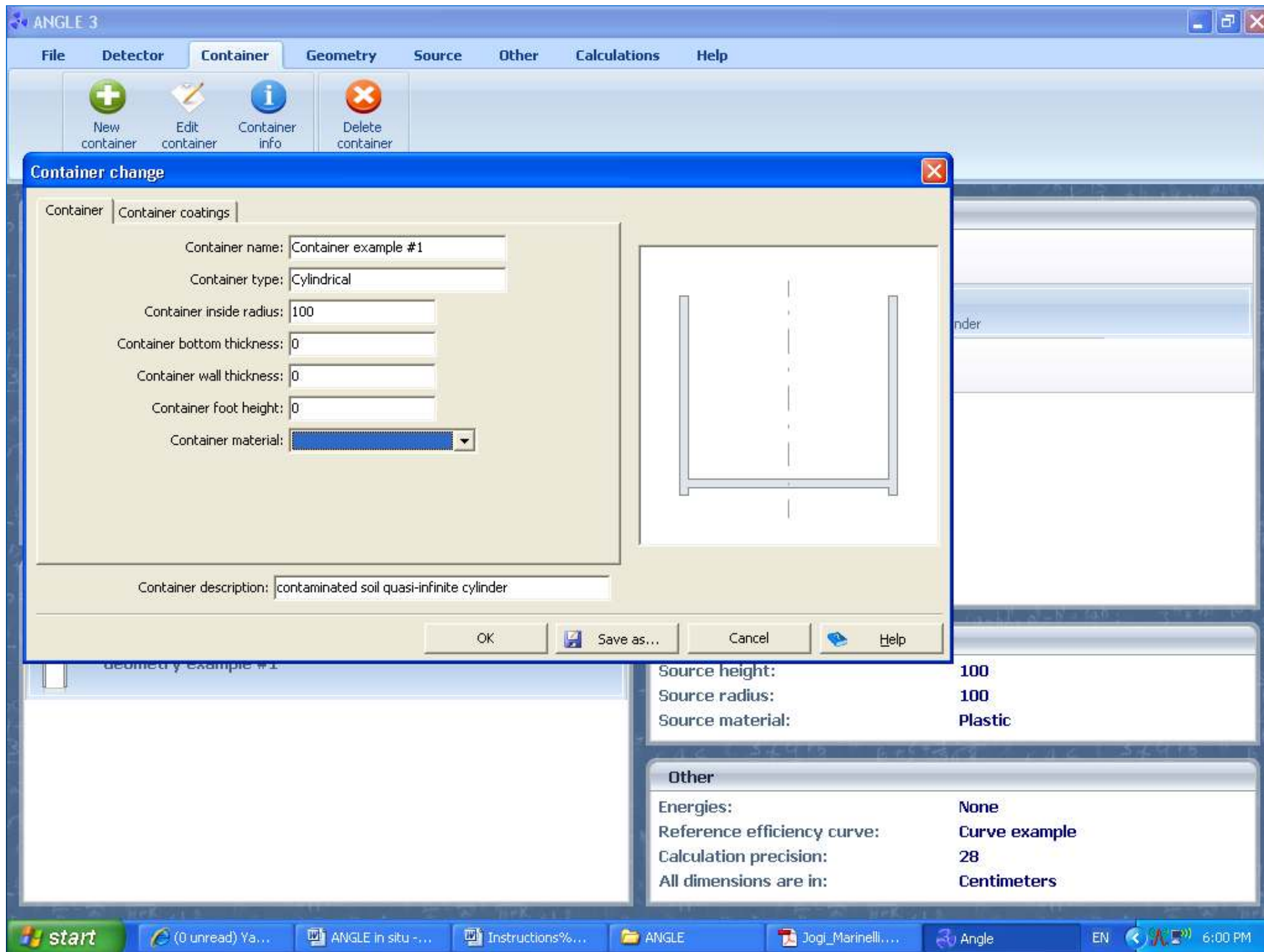


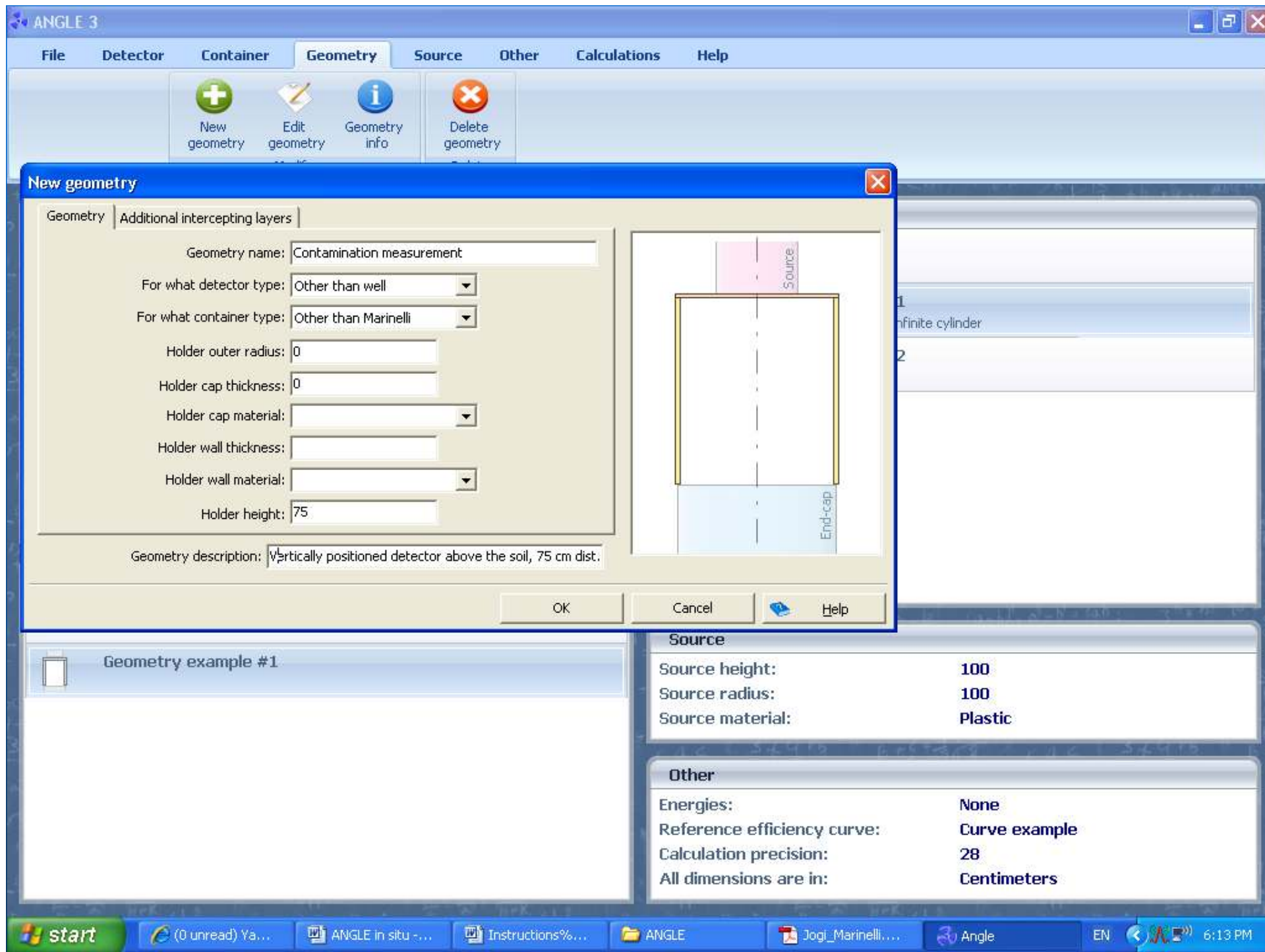


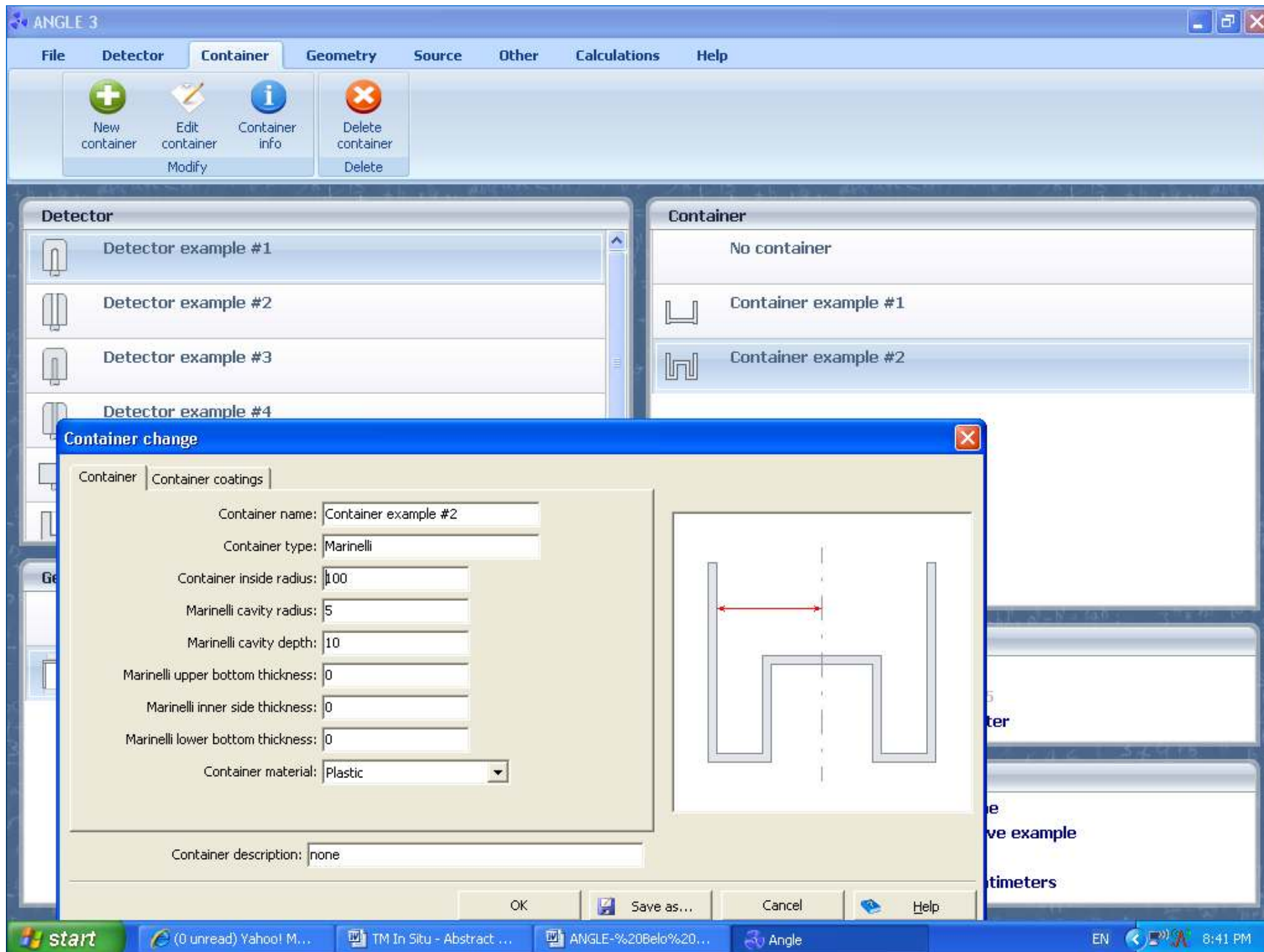














## Introduction of Marinelli effective solid angles for correcting the calibration of NaI(Tl) field gamma-ray spectrometry in TL/OSL dating

F. De Corte,<sup>1\*</sup> S. M. Hossain,<sup>1</sup> S. Jovanović,<sup>2</sup> A. Dlabáč,<sup>2</sup> A. De Wispelaere,<sup>1</sup>  
D. Vandenberghe,<sup>1</sup> P. Van den Haute<sup>3</sup>

<sup>1</sup> Lab. Anal. Chem., Inst. Nucl. Sci., Ghent University, Proefuinststraat 86, B-9000 Gent, Belgium

<sup>2</sup> University of Montenegro, Fac. of Sci., Cetinjski put bb, YU-81000 Podgorica, Yugoslavia

<sup>3</sup> Geological Institute, Ghent University, Krijgslaan 281, B-9000 Gent, Belgium

(Received February 15, 2003)

A study is made of the corrections that are needed in the evaluation of the annual radiation dose, for use in TL/OSL-dating, via NaI(Tl) field gamma-ray spectrometry (monitoring of K, Th and U), calibrated via voluminous blocks that are simulating the Auger hole measuring conditions. Two cases are considered: the “Heidelberg” granite calibration block, which was found to be “quasi-infinite”, and the “Oxford” concrete calibration blocks, for which “effective” concentrations of elements are reported so as to account for their “non-infiniteness”. The calculations, via the software package ANGLE, are based on the concept of effective solid angles for Marinelli geometries.

### Introduction

In the dating technique via thermally or optically stimulated luminescence,<sup>1,2</sup> the TL/OSL-age is given by:

$$\text{TL/OSL - age} = \frac{\text{TL/OSL - signal}}{\text{Annual radiation dose} \times \text{Sensitivity}} \quad (1)$$

$$[\text{conc}_{\text{K,Th,U}}]_{\text{field}} = [\text{conc}_{\text{K,Th,U}}]_{\text{block}} \times \frac{[\text{cps}_{\text{K,Th,U}}]_{\text{field}}}{[\text{cps}_{\text{K,Th,U}}]_{\text{block}}} \quad (2)$$

In the present work, this is investigated for the “Heidelberg” calibration block, for which it was thus far assumed that the shape holds. Additionally,



ELSEVIER

Available online at [www.sciencedirect.com](http://www.sciencedirect.com)

Nuclear Instruments and Methods in Physics Research A 572 (2007) 739–744

**NUCLEAR  
INSTRUMENTS  
& METHODS  
IN PHYSICS  
RESEARCH**  
Section A

[www.elsevier.com/locate/nima](http://www.elsevier.com/locate/nima)

# Contribution of $^{210}\text{Pb}$ bremsstrahlung to the background of lead shielded gamma spectrometers

D. Mrđa\*, I. Bikit, M. Vesković, S. Forkapić

Department of Physics, Faculty of Sciences, University of Novi Sad, Novi Sad 21 000, Trg Dositeja Obradovića 4, Serbia and Montenegro

Received 9 August 2006; received in revised form 18 December 2006; accepted 22 December 2006

Available online 3 January 2007

## Abstract

Lead, which is often used as a shielding material, contains  $^{210}\text{Pb}$  ( $T_{1/2} = 22.3$  y). The 46.54 keV  $\gamma$ -intensity of  $^{210}\text{Pb}$  can be easily reduced by an inner lining, but the bremsstrahlung caused by the  $\beta$ -decay of its daughter,  $^{210}\text{Bi}$ , with a maximal electron energy of 1.16 MeV, will contribute to the gamma detector background. The spectrum of this bremsstrahlung is calculated by numerically fitting the  $\beta$ -spectrum and integrating the Koch–Motz formula. The absorption of the bremsstrahlung in the lead and detection efficiencies for the HPGe detector are calculated by the effective solid angle algorithm, using corrections for the photopeak/Compton ratio of cross-sections in Ge. By comparison with the measured background spectrum, it is shown that, for the lead with 25 Bq/kg of  $^{210}\text{Pb}$  up to 500 keV of gamma spectrum, the bremsstrahlung contribution to the background is about 20% for our surface-based detector system. Also, we compared our calculations with a Monte Carlo simulation of another detector system with a shield containing 1 Bq/kg of  $^{210}\text{Pb}$  and found that our analytical method gives a value of roughly two times higher than the Monte Carlo one for the total bremsstrahlung contribution. The quality of the analytical semi-empirical method is proved by the reasonable agreement with the experimental results.



606 (2009) 49.pdf - Adobe Reader

File Edit View Document Tools Window Help



495 (1 of 6) Find 105%

Nuclear Instruments and Methods in Physics Research A 606 (2009) 495–500

Contents lists available at ScienceDirect

**Nuclear Instruments and Methods in Physics Research A**

journal homepage: [www.elsevier.com/locate/nima](http://www.elsevier.com/locate/nima)

**Production of X-rays by cosmic-ray muons in heavily shielded gamma-ray spectrometers**

I. Bikit<sup>a,\*</sup>, D. Mrda<sup>a</sup>, I. Anicin<sup>b</sup>, M. Veskovc<sup>a</sup>, J. Slivka<sup>a</sup>, M. Krmar<sup>a</sup>, N. Todorovic<sup>a</sup>, S. Forkapic<sup>a</sup>

<sup>a</sup> University of Novi Sad, Faculty of Sciences, Department of Physics, Trg Dositeja Obradovica 4, 21000 Novi Sad, Serbia  
<sup>b</sup> Faculty of Physics, University of Belgrade, Studentski Trg 12, 11000 Belgrade, Serbia

**ARTICLE INFO**

*Article history:*  
Received 6 January 2009  
Received in revised form 22 May 2009  
Accepted 22 May 2009  
Available online 30 May 2009

**Keywords:**  
Cosmic-ray muons  
X-rays production  
Lead shield of Ge detector  
Secondary particles induced by muons  
Coincidence spectrum  
Effective cross-sections

**ABSTRACT**

Cosmic-ray (CR) muons both directly and indirectly contribute to the spectra of heavily shielded High Purity Germanium (HPGe) detectors, even in deep underground laboratories. Heavy elements are frequently used as the detector components or are occasionally placed close to the detector endcap, and their characteristic X-rays induced by cosmic-ray muons contribute to the low-energy region of the HPGe detector spectra. We study the production of X-rays in tungsten, gold and lead by cosmic-ray muons on the ground level, by means of a coincidence system consisting of a plastic scintillation detector and an extended range HPGe detector placed inside a 12-cm-thick lead shield. In this typical low-background arrangement, the shield with total mass of 725 kg acts as a source of secondary particles induced by CR muons. X-rays that originate from direct interactions of muons with the target material, the yield of which may be reliably estimated by Monte Carlo simulations, are excluded by this experimental setup, and only X-rays of W, Pb and Au samples produced by all secondaries from muon interactions with the lead shield are present in the HPGe spectra. The production rate of  $K_{\alpha}$  X-rays per unit mass of all the elements studied ( $74 < Z < 82$ ) is found to be close to  $7 \times 10^{-4} \text{ g}^{-1} \text{ s}^{-1}$ . This

start ANGLE in situ - ppp (0 unread) Yahoo! ... ANGLE in situ - pap... ANGLE 606 (2009) 49.pdf ... EN 12:07 PM



PERGAMON

Applied Radiation and Isotopes 56 (2002) 703–709

**Applied  
Radiation and  
Isotopes**

[www.elsevier.com/locate/apradiso](http://www.elsevier.com/locate/apradiso)

## Reliability of two calculation codes for efficiency calibrations of HPGe detectors

K. Abbas\*, F. Simonelli, F. D'Alberti, M. Forte, M.F. Stroosnijder

*Institute for Health and Consumer Protection, European Commission, Joint Research Centre, Cyclotron TP 500, I-21020 Ispra, Italy*

Received 27 November 2000; received in revised form 15 November 2001; accepted 19 November 2001

### Abstract

This paper reports the reliability of efficiency calibrations for  $\gamma$ -ray detectors using the calculation codes ANGLE and LabSOCS. For experimental verification, three HPGe detectors under various laboratory geometry configurations were used for this study. An overall comparison between experimental and calculated efficiency calibration curves is presented and comments on the various error sources affecting the final results are given. The deviations are generally below 10%, which could be acceptable for many applications. © 2002 Elsevier Science Ltd. All rights reserved.

**Keywords:** ANGLE code; LabSOCS code; Efficiency calibration codes;  $\gamma$ -ray spectrometry; HPGe detectors



Contents lists available at ScienceDirect

## Applied Radiation and Isotopes

journal homepage: [www.elsevier.com/locate/apradiso](http://www.elsevier.com/locate/apradiso)

## Testing efficiency transfer codes for equivalence

T. Vidmar<sup>a,\*</sup>, N. Çelik<sup>a,b</sup>, N. Cornejo Díaz<sup>c</sup>, A. Dlabac<sup>d</sup>, I.O.B. Ewa<sup>e</sup>, J.A. Carrazana González<sup>c</sup>,  
M. Hult<sup>a</sup>, S. Jovanović<sup>d</sup>, M.-C. Lépy<sup>f</sup>, N. Mihaljević<sup>d</sup>, O. Sima<sup>g</sup>, F. Tzika<sup>h</sup>, M. Jurado Vargas<sup>i</sup>,  
T. Vasilopoulou<sup>h,j</sup>, G. Vidmar<sup>k</sup>

<sup>a</sup> European Commission, JRC, IRMM, Geel, Belgium<sup>b</sup> Karadeniz Technical University, Trabzon, Turkey<sup>c</sup> Centro de Protección e Higiene de las Radiaciones, La Habana, Cuba<sup>d</sup> University of Montenegro, Podgorica, Montenegro<sup>e</sup> Ahmadu Bello University, Zaria, Nigeria<sup>f</sup> Commissariat à l'Énergie Atomique, Gif sur Yvette Cedex, France<sup>g</sup> Bucharest University, Bucharest, Romania<sup>h</sup> National Centre for Scientific Research 'Demokritos', Athens, Greece<sup>i</sup> University of Extremadura, Badajoz, Spain<sup>j</sup> National Technical University of Athens, Athens, Greece<sup>k</sup> University Rehabilitation Institute, Ljubljana, Slovenia

## ARTICLE INFO

## Article history:

Received 15 June 2009

Received in revised form

28 September 2009

Accepted 12 October 2009

## ABSTRACT

Four general Monte Carlo codes (GEANT3, PENELOPE, MCNP and EGS4) and five dedicated packages for efficiency determination in gamma-ray spectrometry (ANGLE, DETEFF, GESPECOR, ETNA and EFFTRAN) were checked for equivalence by applying them to the calculation of efficiency transfer (ET) factors for a set of well-defined sample parameters, detector parameters and energies typically encountered in environmental radioactivity measurements. The differences between the results of the different codes



ANGLE v2.1 paper NIM A.pdf - Adobe Reader


File Edit View Document Tools Window Help

1 / 7 Find 105%


ARTICLE IN PRESS

Nuclear Instruments and Methods in Physics Research A (■■■■) ■■■–■■■

Contents lists available at ScienceDirect

 Nuclear Instruments and Methods in Physics Research A

journal homepage: [www.elsevier.com/locate/nima](http://www.elsevier.com/locate/nima)



## ANGLE v2.1—New version of the computer code for semiconductor detector gamma-efficiency calculations

S. Jovanovic<sup>a,\*</sup>, A. Dlabac<sup>a</sup>, N. Mihaljevic<sup>b</sup>

<sup>a</sup> University of Montenegro, Faculty of Natural Sciences, Department of Physics, Dz. Vasingtona bb, Podgorica, Montenegro  
<sup>b</sup> University of Montenegro, Maritime Faculty, Department of Mathematics, Dobrota 36, Kotor, Montenegro

---

### ARTICLE INFO

**Keywords:**  
ANGLE software  
Efficiency transfer method  
Efficiency calibration  
Semiconductor detectors  
Gamma-spectrometry

### ABSTRACT

New version of the commercially available ANGLE software for semiconductor detector gamma-efficiency calculations is presented. ANGLE allows for accurate determination of the activities of gamma spectroscopic samples for which no “replicate” standard exists, in terms of geometry and matrix. A semi-empirical (“efficiency transfer”) approach is applied, based on the effective solid angle calculations. Advantages of both absolute (Monte Carlo) and relative (calibrated-source-based) methods are combined—while minimizing potential for systematic errors in the former and reducing practical limitations of the latter. ANGLE is broadly applicable, accounting for most of counting arrangements in gamma-spectrometry practice (in respect to detector types and configuration, source shapes and volumes, matrix composition, source-to-detector distance, etc.). Besides the years of practical utilization in many gamma-spectrometry laboratories, accuracy of the software is successfully tested in a recent IAEA-organized intercomparison exercise—ANGLE scored 0.65% average deviation from the exercise mean for  $E_\gamma > 20\text{keV}$  energies.

© 2010 Elsevier B.V. All rights reserved.

start ANGLE i... {0 unre... ANGLE i... ANGLE 606 (20... Paper o... ET pap... ANGLE ... EN 12:11 PM

# ANGLE v3.0

[http://www.dlabac.com/angle/files/angle\\_setup.exe](http://www.dlabac.com/angle/files/angle_setup.exe)

<http://www.ortec-online.com/software/angle.htm>

bobo\_jovanovic@yahoo.co.uk, adlabac@t-com.me

The background is a solid dark blue. It features several abstract geometric elements: a large, faint, light blue circular shape in the center, and two large, light blue curved shapes on the left and right sides. A horizontal band of dark blue is at the top. A thin, light blue grid pattern is visible in the upper left quadrant.

*Thanks!*



**Montenegro**

*- a great heart of the Mediterranean -*







Brijuni - Bora

(c) 2003 Stevan Kordić

































